

Structure and Solution Behavior of a Series of Classical and Nonclassical Rhenium Hydride Complexes

Dmitry G. Gusev, Daniel Nietlispach, Igor L. Eremenko, and Heinz Berke*

Anorganisch-Chemisches Institut der Universität Zürich, Winterthurerstrasse 190, CH-8057 Zürich, Switzerland

Received February 19, 1993

A series of nonclassical rhenium dihydrogen complexes, $\text{Re}(\text{H}_2)(\text{CO})_n(\text{PMe}_3)_{5-n}^+$ ($n=1-3$), $\text{Re}(\text{H}_2)(\text{H})_2(\text{CO})-(\text{PMe}_3)_3^+$, and $\text{ReH}(\text{H}_2)(\text{CO})(\text{NO})(\text{PPr}^i)_2^+$ and their isotopomers are prepared by the protonation of the corresponding mono-, di-, or trihydride or deuteride complexes at low temperature and are characterized by NMR methods. The stability, structure, and solution behavior are studied. Due to a subsequent conversion of the nonclassical $\text{Re}(\text{H}_2)(\text{CO})(\text{PMe}_3)_4^+$ compound into the previously reported corresponding classical dihydride complex $\text{ReH}_2(\text{CO})-(\text{PMe}_3)_4^+$ an isolable protonation product is obtained in the case of $\text{Re}(\text{H}_2)(\text{CO})(\text{PMe}_3)_4^+$. The other representatives of dihydrogen complexes are very labile and decompose at temperatures above 230 K. $\text{Re}(\text{H}_2)(\text{H})_2(\text{CO})(\text{PMe}_3)_3^+$ exists as an equilibrium mixture with its classical tautomer $\text{ReH}_4(\text{CO})(\text{PMe}_3)_3^+$. A variable-temperature study of this transformation reveals the following thermodynamic parameters: $\Delta H = -1.05 \pm 0.1$ kcal/mol and $\Delta S = -2.3 \pm 0.6$ eu. In addition using dynamic NMR methods the exchange process between the dihydrogen and the hydride positions of the nonclassical tautomer $\text{Re}(\text{H}_2)(\text{H})_2(\text{CO})(\text{PMe}_3)_3^+$ is investigated. A kinetic isotope effect ($k_{\text{H}}/k_{\text{D}} = 2$ at 183 K) is observed. Thus, H–H bond cleavage participates in the rate-determining step. Possible mechanisms are discussed on the basis of kinetic and spectroscopic data. $\text{ReH}(\text{CO})_2(\text{PMe}_3)_3$, $[\text{ReH}_2(\text{CO})(\text{PMe}_3)_4][\text{BPh}_4]$, and $\text{ReH}_3(\text{CO})(\text{PMe}_3)_3$ were characterized by X-ray structure analyses: $\text{ReH}(\text{CO})_2(\text{PMe}_3)_3$, space group $P2_12_12_1$, $a = 14.249(8)$ Å, $b = 16.067(6)$ Å, $c = 16.466(7)$ Å, $Z = 8$ (two independent molecules), $R = 0.069$, $R_w = 0.077$ for 3234 reflections with $F > 6\sigma(F)$; $[\text{ReH}_2(\text{CO})(\text{PMe}_3)_4][\text{BPh}_4]$, space group $P2_12_12_1$, $a = 10.000(5)$ Å, $b = 13.197(6)$ Å, $c = 30.891(13)$ Å, $Z = 4$, $R = 0.064$, $R_w = 0.073$ for 3562 reflections with $F > 6\sigma(F)$; $\text{ReH}_3(\text{CO})-(\text{PMe}_3)_3$, space group $Pna2_1$, $a = 20.423(4)$ Å, $b = 11.475(3)$ Å, $c = 15.444(4)$ Å, $Z = 8$ (two independent molecules), $R = 0.057$, $R_w = 0.057$ for 2993 reflections with $F > 6\sigma(F)$.

Introduction

Recently we have prepared a series of manganese and rhenium hydride complexes and studied the selective and nonselective T_1 relaxation of the H ligands to determine the M–H bond lengths and the reliability of the structural information derived from the relaxation data.^{1a} Some of the compounds $\text{ReH}(\text{CO})_n(\text{PMe}_3)_{5-n}$, $\text{ReH}_3(\text{CO})(\text{PMe}_3)_3$, and $\text{ReH}_2(\text{CO})(\text{NO})(\text{PPr}^i)_2$ have provided opportunity to attempt preparation of a series of corresponding dihydrogen complexes by protonation^{1b} allowing a comparative study of their stability, structure, and solution behavior. Another interesting aspect of our investigations is the comparison of the reported tautomeric equilibria between protonation products of related complexes $\text{ReH}(\text{CO})_2(\text{PMe}_2\text{Ph})_3$ and $\text{ReH}_3(\text{CO})(\text{PMe}_2\text{Ph})_3$.² The electronic and steric factors governing such equilibria are very subtle and not easily unraveled. Thus, ligand variation may be an appropriate tool to tackle this problem experimentally.

For such rhenium complexes formation of nonclassical and, in two cases, classical hydrides has been found. This work reports their structural and dynamic properties investigated by NMR and X-ray.

Experimental Section

All NMR measurements were performed on a Varian Gemini 300 instrument in solutions of CD_2Cl_2 or CH_2Cl_2 predried over molecular sieves. ^1H and ^2H NMR spectra were referenced to the resonance of CH_2Cl_2 (δ 5.32). ^{31}P chemical shifts were externally referenced to 85% H_3PO_4 . The conventional inversion–recovery method (180– τ –90) was

used to determine T_1 . The calculations of the relaxation times were made by applying the nonlinear three-parameter fitting routine of the spectrometer.

The studied solutions had concentrations of the complexes of 40–50 mg mL⁻¹. As a rule, freezing points of solutions containing acids were found to be lower than that of the pure solvent by 10–15°. Calibration of the temperature controller of the spectrometer against a methanol sample revealed a difference between the dial temperature and that in the probe of less than 3° below –70 °C. Corrected temperature values were used in calculations of kinetic and thermodynamic parameters.

$\text{ReH}(\text{CO})_3(\text{PMe}_3)_2$, $\text{ReH}(\text{CO})_2(\text{PMe}_3)_3$, $\text{ReH}(\text{CO})(\text{PMe}_3)_4$, $\text{ReH}_3(\text{CO})(\text{PMe}_3)_3$, and $\text{ReH}_2(\text{CO})(\text{NO})(\text{PPr}^i)_2$ were prepared by reported procedures.¹

Cationic complexes $\text{Re}(\text{H}_2)(\text{CO})_3(\text{PMe}_3)_2^+$ (1), $\text{Re}(\text{H}_2)(\text{CO})_2-(\text{PMe}_3)_3^+$ (2), $\text{Re}(\text{H}_2)(\text{CO})(\text{PMe}_3)_4^+$ (3a), $\text{Re}(\text{H})_2(\text{H}_2)(\text{CO})(\text{PMe}_3)_3^+$ (4a), $\text{ReH}_4(\text{CO})(\text{PMe}_3)_3^+$ (4b), and $\text{ReH}(\text{H}_2)(\text{CO})(\text{NO})(\text{PPr}^i)_2^+$ (5) studied in this work were too unstable to be isolated. Thus, they were prepared in situ in NMR tubes by protonation of the corresponding mono-, di-, or trihydride complexes with $\text{CF}_3\text{SO}_3\text{H}$ or CF_3COOH according to the following procedure: 25–30 mg of the starting compound was dissolved in 0.6 mL of CD_2Cl_2 . The solution was transferred into a 5-mm NMR tube sealed onto a glass Kontes valve with a Teflon stopcock. This apparatus was attached to a vacuum line, and the solution was carefully degassed by the conventional freeze–pump–thaw technique. After cooling of the sample solution to –95 °C, the acid (15 μL , 3–4-fold excess) was added with a microsyringe under nitrogen purge. The sample tube was then evacuated, flame sealed, and transferred into the precooled probe of the spectrometer.

$\text{Re}(\text{H}_2)(\text{CO})_3(\text{PMe}_3)_2^+$ (1). ^1H NMR (CD_2Cl_2 , 181 K): δ 1.89 (br s, CH_3), –4.70 (br s, $\Delta = 94$ Hz, $\text{Re}(\text{H}_2)$). ^{31}P (^1H) NMR (CD_2Cl_2 , 181 K): δ –41.2. ^1H T_1 relaxation measurements revealed a $T_{1\text{min}}$ value of 6.7 ms for the dihydrogen resonance at 183 K. A 1:1:1 triplet ($J(\text{H}–\text{D}) = 33$ Hz) was observed in the hydride region of the ^1H NMR spectrum at δ –4.93 for $\text{Re}(\text{HD})(\text{CO})_3(\text{PMe}_3)_2^+$ prepared by the reaction of $\text{ReH}(\text{CO})_3(\text{PMe}_3)_2$ with CF_3COOD .

$\text{Re}(\text{H}_2)(\text{CO})_2(\text{PMe}_3)_3^+$ (2). ^1H NMR (CD_2Cl_2 , 193 K): δ 1.77 (br s, CH_3 , 18H), 1.59 (d, $^2J_{\text{HP}} = 7.4$ Hz, CH_3 , 9H), –4.73 (br s, $\Delta = 58$

- (1) (a) Gusev, D. G.; Nietlispach, D.; Vymenits, A. B.; Bakhmutov, V. I.; Berke, H. *Inorg. Chem.*, in press. (b) Jessop, P. G.; Morris, R. H. *Coord. Chem. Rev.* **1992**, *121*, 155 and references therein.
- (2) (a) Luo, X.-L.; Crabtree, R. H. *J. Chem. Soc., Chem. Commun.* **1990**, 189. (b) Luo, X.-L.; Crabtree, R. H. *J. Am. Chem. Soc.* **1990**, *112*, 6912. (c) Luo, X.-L.; Michos, D.; Crabtree, R. H. *Organometallics* **1992**, *11*, 237.

H₂, Re(H₂)). ³¹P(1H) NMR (CD₂Cl₂, 193 K): δ -44.5 (a well-resolved non-first-order AB₂ pattern resulting from a small difference in the chemical shifts, δ(A) and δ(B)). For the dihydrogen resonance an ¹H T_{1min} time of 8.2 ms was found at 183 K. The HD ligand of Re(HD)-(CO)₂(PMe₃)₃⁺ prepared by using CF₃COOD was characterized by a J(H-D) coupling constant of 33.7 Hz.

Re(H₂)(CO)(PMe₃)₄⁺ (3a). ¹H NMR (CD₂Cl₂, 213 K): δ 1.70 (br s, CH₃, 18H), 1.62 (d, ²J_{HP} = 7.9 Hz, CH₃, 9H), 1.45 (d, ²J_{HP} = 6.5 Hz, CH₃, 9H), -6.45 (br s, Δ = 35 Hz, Re(H₂)). ³¹P(1H) NMR (CD₂Cl₂, 213 K): δ -39.8 (q, ²J_{PP} = 27.2 Hz, 1P), -48.1 (a resolved non-first-order pattern resulting from a small (<0.7 ppm) difference in the chemical shifts, δ(B) and δ(C), in the ABC₂ phosphorus spin system). An ¹H resonance of the HD ligand of Re(HD)(CO)(PMe₃)₄⁺ was observed at 223 K at δ -6.49 as a well-resolved triplet of doublets of quartets (J_{HD} = 27.7 Hz, ²J_{HP} = 9.4, 4.7 Hz). A doublet with the same H-D coupling was also observed in the ²H NMR spectrum of this complex together with a singlet at δ -6.44 due to the isotopomer Re(D₂)(CO)(PMe₃)₄⁺. An ¹H T_{1min} time of 9 ms was measured at -183 K for the dihydrogen ligand of 3a.

ReH₂(CO)(PMe₃)₄⁺ (3b). A solution of ReH(CO)(PMe₃)₄ (0.51 g, 0.98 mmol) in 20 mL of CH₂Cl₂ was protonated with CF₃COOH (80 μL, 0.98 mmol) at -20 °C. After 5 min, NaBPh₄ (0.33 g, 0.98 mmol) was added and the solution was allowed to warm up to ambient temperature. After 1 h addition of 50 mL of diethyl ether resulted in precipitation of a white microcrystalline powder. The solid was filtered out, washed with cold diethyl ether (2 × 20 mL), and dried in vacuo. ¹H NMR (CD₂Cl₂, 233 K): δ 1.84 (d, ²J_{HP} = 9.9 Hz, CH₃, 9H), 1.71 (d, ²J_{HP} = 7.9 Hz, CH₃, 18H), 1.50 (d, ²J_{HP} = 7.2 Hz, CH₃, 9H), -5.89 (m, ReH₂). ³¹P(1H) NMR (CD₂Cl₂, 213 K): δ -21.5 (td, ²J_{PP} = 22.3, 14.9 Hz, 1P), -44.5 (dd, ²J_{PP} = 26.8, 22.3 Hz, 2P), -50.7 (td, ²J_{PP} = 26.8, 14.9 Hz, 1P). At 213 K the hydride-coupled ³¹P NMR spectrum of 3b is characterized by an XYZZ' part of an AA'XYZZ' (A, A', ¹H; X, Y, Z, Z', ³¹P) spin system. By simulation of the spectrum the following values for the coupling constants were obtained: ²J_{XA} = ²J_{XA'} = ±44.7 Hz, ²J_{YA} = ²J_{YA'} = ∓20.7 Hz, ²J_{ZA} = ²J_{ZA'} = ±54 Hz, ²J_{ZA'} = ²J_{ZA} = ∓2 Hz, ²J_{ZZ'} = ±55 Hz; δ -21.5 (X), -50.7 (Y), -44.5 (Z, Z'). T_{1min}(ReH₂) = 210 ms (183 K).

Re(H₂)₂(CO)(PMe₃)₃⁺ (4a). ¹H NMR (CD₂Cl₂, 168 K): δ 1.72 (br s, CH₃), -5.53 (apparent triplet, J_{HP} = 46 Hz, Re(H)₂), -6 (vbr s, Re(H₂)). ³¹P(1H) NMR (CDCl₂, 163 K): δ -21.1 (t, ²J_{PP} = 26 Hz, 1P), -39.8 (d, 2P). The hydride-coupled ³¹P NMR spectrum of 4a at 163 K is the XY'Y' part of an AA'XY'Y' (A, A', ¹H; X, Y, Y', ³¹P) spin system with the following coupling constants: ²J_{XA} = ²J_{XA'} = 44.0 Hz, ²J_{YA} = ²J_{YA'} = 47.0 Hz, ²J_{YA'} = ²J_{YA} = 0.5 Hz, ²J_{YY'} = 47 Hz; δ -21.1 (X), -39.8 (Y, Y'). T_{1min} (CD₂Cl₂, 168 K): 115 ms (Re(H)₂), 8.3 ms (Re(H₂)). At 168 K the ¹H NMR spectrum of the partially deuterated complex 4a displays an HD ligand resonance at δ -6.04 (J_{HD} = 33.6 Hz).

ReH₄(CO)(PMe₃)₃⁺ (4b). ¹H NMR (CD₂Cl₂, 168 K): δ 1.72 (br s, CH₃), -4.79 (q, ²J_{HP} = 19.3 Hz, ReH₄). ³¹P(1H) NMR (CD₂Cl₂, 168 K): δ -41.5 (t, ²J_{PP} = 16.6 Hz, 1P), -43.3 (d, 2P). T_{1min}(ReH₄) = 130 ms (170 K).

ReH(H₂)(CO)(NO)(PPR₃)₂⁺ (5). ¹H NMR (CD₂Cl₂, 158 K): δ 2.44 (br s, CH), 1.19 (br s, CH₃), -2 (vbr s, Re(H₂)), -2.46 (t, ²J_{HP} = 24.4 Hz, ReH). A small triplet (δ 2.67, ²J_{HP} = 25.5 Hz) was present in all low-temperature ¹H NMR spectra of 5. ³¹P(1H) NMR (CD₂Cl₂, 158 K): δ 39.0 (s, 2P). The phosphorus resonance turned into a doublet when the phosphane protons were selectively decoupled at 158 K. T_{1min} = 7.3 ms (193 K) for the averaged resonance of the H and H₂ ligands. A T₁ time of 68 ms was measured for the triplet resonance due to ReH at 158 K.

Crystal Structure Determinations. Single crystals of ReH(CO)₂(PMe₃)₃ and ReH₃(CO)(PMe₃)₃ were grown from hexane solutions and from CH₂Cl₂/Et₂O in the case of [ReH₂(CO)(PMe₃)₄][BPh₄] at -30 °C. In all cases colorless prisms formed.

ReH(CO)₂(PMe₃)₃. A crystal of the approximate dimensions 0.7 × 0.5 × 0.3 mm glued to a glass fiber using epoxy resin was mounted on a goniometer head and centered on a Siemens R 3m/v diffractometer (Mo Kα, λ = 0.710 73 Å for all investigated complexes). The unit cell parameters were determined and refined from a set of 24 equivalent reflections (28° < 2θ < 30°) well distributed in reciprocal space. Inspection of the indices showed that reflections having 00l, l = 2n + 1; 0k0, k = 2n + 1; and h00, h = 2n + 1 were systematically absent consistent with the space group P2₁2₁2₁. Data were collected through ω-2θ scans over the range 5.0° < 2θ < 46° with variable scan speeds (2.49-14.65°/min) and a 0.8° scan width. There standard reflections, measured after every 97 collected reflections, showed no decay in intensity. Details of

Table I. Crystallographic Data for ReH(CO)₂(PMe₃)₃, [ReH₂(CO)(PMe₃)₄][BPh₄], and ReH₃(CO)(PMe₃)₃

| chem formula | C ₁₁ H ₂₈ O ₂ P ₃ Re | C ₃₇ H ₅₈ BOP ₄ Re | C ₁₀ H ₃₀ OP ₃ Re |
|---|--|--|--|
| fw | 471.4 | 839.7 | 445.5 |
| space group | P2 ₁ 2 ₁ 2 ₁ (No. 19) | P2 ₁ 2 ₁ 2 ₁ (No. 19) | Pna2 ₁ (No. 33) |
| a, Å | 14.249(8) | 10.000(5) | 20.423(4) |
| b, Å | 16.067(6) | 13.197(6) | 11.475(3) |
| c, Å | 16.466(7) | 30.891(13) | 15.444(4) |
| V, Å ³ | 3770(3) | 4076(3) | 3619(2) |
| Z | 8 ^a | 4 | 8 ^a |
| ρ _{calcd} , g cm ⁻³ | 1.661 | 1.368 | 1.635 |
| T, °C | 24 | -40 | -60 |
| μ, cm ⁻¹ | 67.78 | 32.00 | 70.51 |
| 2θ range, deg | 5-46 | 5-52 | 5-52 |
| min-max transm coeff | 0.0377-0.1761 | | |
| no. of unique data | 3916 | 4450 | 3515 |
| no. of obsd data with F _o ≥ 6σ(F _d) | 3234 | 3562 | 2993 |
| R ^b | 0.069 | 0.064 | 0.057 |
| R _w ^c | 0.077 | 0.073 | 0.057 |

^a Two independent molecules in the unit cell. ^b Σ|F_o - F_d|/ΣF_o. ^c [Σw(|F_o - F_d|)²/Σw|F_o|²]^{1/2}.

crystal parameters, data collection, and structure refinement are given in Table I. A semiempirical absorption correction (μ = 67.78 cm⁻¹) was employed which gave a good agreement with 10 intense reflections as observed at several different values of φ. The structure was solved using the SHELXTL PLUS program package. The rhenium atoms of the two independent molecules were located by direct methods. Standard Fourier methods were used to locate the remaining non-hydrogen atoms in the molecule. The hydrogen atoms of the PMe₃ ligands were included as fixed contributors in the calculations of atomic positions. The refinement of the non-hydrogen atoms in an anisotropic approximation and with fixed hydrogen atoms of the PMe₃ ligands was followed by a difference Fourier map, which revealed the positions of the isotropically refined hydride atoms in both independent molecules. The final cycles of least-squares refinement applying a unit weighting scheme gave R = 6.93% and R_w = 7.67%. The function minimized in the least-squares calculations was Σw(F_o - F_d)². A largest peak in the difference Fourier map was a rhenium residual of 2.62 e Å⁻³.

[ReH₂(CO)(PMe₃)₄][BPh₄]. A crystal of suitable size (0.3 × 0.3 × 0.2 mm) was mounted using epoxy glue. It was transferred to a goniostat and cooled to -40 °C for characterization and data collection. A systematic search of a limited hemisphere in reciprocal space revealed symmetry and systematic absence of reflections having 00l, l = 2n + 1; 0k0, k = 2n + 1; and h00, h = 2n + 1 corresponding to the orthorhombic space group P2₁2₁2₁.

The structure was solved by a usual combination of direct methods and Fourier techniques using the SHELXTL PLUS program package. After isotropic refinement of all non-hydrogen atoms an absorption correction (μ = 32.00 cm⁻¹) was employed using the DIFABS program. The following anisotropic refinement of the non-hydrogen atoms with fixed hydrogen atoms of the PMe₃ ligands gave R = 6.54%. At this stage a difference Fourier map led to the positions of the hydride atoms, which were refined isotropically. The final cycles of least-squares refinement applying a unit weighting scheme gave R = 6.42% and R_w = 7.26%. A difference Fourier map exhibited maximum and minimum residues (1.26 and -1.58 e Å⁻³) in the vicinity of the rhenium atom.

ReH₃(CO)(PMe₃)₃. A crystal of suitable size (0.7 × 0.1 × 0.1 mm) was mounted on top of a glass fiber with 15-min epoxy resin. Accurate unit cell parameters were obtained by means of a least-squares analysis of 24 equivalent reflections (22 < 2θ < 26°). Inspection of the data showed that reflections having 0kl, k + l = 2n + 1, and h0l, h = 2n + 1, were systematically absent, consistent with the space group Pna2₁ or Pnam. Intensity data were collected through ω-2θ scans over the range 5 < 2θ < 52° with variable scan speeds (2.49-14.65°/min) and a 0.75 scan width at -60 °C. The structure was solved using the SHELXTL PLUS program package. A solution of the experimental data in the space group Pnma by direct methods or by a Patterson map resulted in positions of two independent Re atoms on the crystallographic m plane. Further localization of non-hydrogen atoms revealed a strong disordering of all PMe₃ ligands and of the CO group in the molecular units. This observation forced us to solve the structure in the space group Pna2₁. The Re atoms of the two independent molecules were determined by direct

Table II. Atomic Coordinates ($\times 10^4$) and Equivalent Isotropic Displacement Coefficients ($\text{\AA}^2 \times 10^3$) for $\text{ReH}(\text{CO})_2(\text{PMe}_3)_3$

| | <i>x</i> | <i>y</i> | <i>z</i> | <i>U</i> (eq) ^a |
|-------|----------|------------|-----------|----------------------------|
| Re(1) | 7713(1) | -8393(1) | 8378(1) | 31(1) |
| Re(2) | 7046(1) | -3885(1) | 9097(1) | 30(1) |
| P(1) | 7479(6) | -8651(5) | 9788(5) | 44(2) |
| P(2) | 7880(8) | -7658(5) | 7135(5) | 53(2) |
| P(3) | 6106(5) | -8792(5) | 8046(5) | 38(2) |
| P(4) | 6350(6) | -4986(5) | 9863(5) | 47(2) |
| P(5) | 7630(6) | -2611(5) | 8558(5) | 45(2) |
| P(6) | 8587(6) | -4527(5) | 9070(6) | 49(2) |
| O(1) | 8309(18) | -10119(15) | 7721(17) | 82(3) |
| O(2) | 9752(20) | -8020(21) | 8741(19) | 106(3) |
| O(3) | 5204(19) | -2933(16) | 9298(18) | 83(3) |
| O(4) | 6571(14) | 4696(17) | 7434(14) | 73(3) |
| C(1) | 8104(21) | -9525(20) | 8035(17) | 52(3) |
| C(2) | 8955(21) | -8155(23) | 8580(19) | 64(3) |
| C(3) | 5908(17) | -3333(20) | 9238(18) | 47(3) |
| C(4) | 6692(16) | -4360(20) | 8046(19) | 46(3) |
| C(11) | 6500(26) | -8241(25) | 10264(20) | 79(3) |
| C(12) | 8365(23) | -8221(25) | 10440(22) | 78(3) |
| C(13) | 7379(32) | -9758(25) | 10145(25) | 114(3) |
| C(21) | 8657(31) | -6873(28) | 7103(29) | 120(3) |
| C(22) | 8267(27) | -8242(25) | 6265(23) | 87(3) |
| C(23) | 6921(26) | -6991(20) | 6797(20) | 78(3) |
| C(31) | 5967(27) | -9215(24) | 7040(21) | 82(3) |
| C(32) | 5598(25) | -9660(23) | 8623(25) | 83(3) |
| C(33) | 5195(22) | -8042(19) | 8120(19) | 56(3) |
| C(41) | 5234(24) | -4712(23) | 10302(23) | 73(3) |
| C(42) | 6900(28) | -5437(25) | 10768(24) | 104(3) |
| C(43) | 6056(24) | -5939(20) | 9301(23) | 74(3) |
| C(51) | 8685(28) | -2145(25) | 9040(27) | 97(3) |
| C(52) | 6710(30) | -1831(28) | 8582(30) | 131(3) |
| C(53) | 7877(34) | -2542(29) | 7457(25) | 123(3) |
| C(61) | 9179(26) | -4457(26) | 8117(24) | 88(3) |
| C(62) | 8693(31) | -5656(26) | 9332(30) | 117(3) |
| C(63) | 9422(24) | -4151(23) | 9846(23) | 79(3) |

^a Equivalent isotropic *U* defined as one-third of the trace of the orthogonalized U_{ij} tensor.

methods. After the localization of the other non-hydrogen atoms by usual Fourier techniques and refinement of their positions in the isotropic approximation, a DIFABS absorption correction was employed. All non-hydrogen atoms were anisotropically refined with fixed hydrogen atoms of the PMe_3 ligands. At this stage the positions of the Re bound hydrogen atoms were extracted from a difference Fourier map. The hydride ligands were refined isotropically. The final cycles of least-squares refinement gave $R = 5.74\%$ and $R_w = 5.71\%$ using the weighting scheme $w^{-1} = \sigma^2(F) + 0.0001F^2$. The largest peak in the difference Fourier map was a rhenium residual of 0.92 e \AA^{-3} .

The crystallographic data and details of the data collection and refinement are given in Table I. Atomic coordinates and selected bond lengths and bond angles of both complexes are listed in Tables II–VII.

Results and Discussion

Preparation and Characterization of $\text{Re}(\text{H}_2)(\text{CO})_3(\text{PMe}_3)_2^+$ (1) and $\text{Re}(\text{H}_2)(\text{CO})_2(\text{PMe}_3)_3^+$ (2). The protonation of the neutral monohydrides $\text{ReH}(\text{CO})_3(\text{PMe}_3)_2$ and $\text{ReH}(\text{CO})_2(\text{PMe}_3)_3$ applying an excess (3–4 equiv) of $\text{CF}_3\text{SO}_3\text{H}$ at -95°C in dichloromethane results in formation of the corresponding cationic dihydrogen complexes $\text{Re}(\text{H}_2)(\text{CO})_3(\text{PMe}_3)_2^+$ (1) and $\text{Re}(\text{H}_2)(\text{CO})_2(\text{PMe}_3)_3^+$ (2). In the hydride region of the ^1H NMR spectra of 1 and 2 single lines at $\delta -4.70$ and -4.73 are observed broadened strongly due to fast relaxation of the protons. The $T_{1\text{min}}$ times measured for these lines (6.7 and 8.2 ms, respectively) are at the low end of the range of values determined for dihydrogen complexes.

For the preparation of ^2H isotopomeric mixtures of 1 and 2 CF_3COOD was used as the protonating agent but otherwise the same conditions as for the syntheses of 1 and 2 were applied. The HD isotopomers for 1 and 2 have large J_{HD} couplings of 33 and 33.7 Hz, respectively. Figure 1 shows the high-field regions of the ^1H and ^2H NMR spectra of partially deuterated 2, clearly demonstrating the well-resolved deuterium resonances for DH

Table III. Atomic Coordinates ($\times 10^4$) and Equivalent Isotropic Displacement Coefficients ($\text{\AA}^2 \times 10^3$) for $[\text{ReH}_2(\text{CO})(\text{PMe}_3)_4][\text{BPh}_4]$

| | <i>x</i> | <i>y</i> | <i>z</i> | <i>U</i> (eq) ^a |
|--------|-----------|-----------|----------|----------------------------|
| Re(1) | 7671(1) | 8471(1) | 9011(1) | 33(1) |
| P(1) | 9540(5) | 9513(4) | 8759(2) | 49(1) |
| P(2) | 6257(6) | 9061(4) | 8414(2) | 46(1) |
| P(3) | 6963(6) | 9780(4) | 9519(2) | 46(1) |
| P(4) | 7227(5) | 6716(3) | 8971(2) | 41(1) |
| O(1) | 9314(20) | 7784(12) | 9786(6) | 96(2) |
| C(1) | 8657(26) | 8001(16) | 9459(8) | 108(2) |
| C(11) | 11043(20) | 9360(17) | 9044(10) | 91(2) |
| C(12) | 10027(25) | 9234(21) | 8178(11) | 162(2) |
| C(13) | 9495(20) | 10883(15) | 8754(6) | 56(2) |
| C(21) | 6289(24) | 8352(20) | 7896(7) | 101(2) |
| C(22) | 4441(20) | 9037(22) | 8519(9) | 97(2) |
| C(23) | 6501(20) | 10320(17) | 8193(8) | 69(2) |
| C(31) | 6119(26) | 10910(18) | 9311(12) | 126(2) |
| C(32) | 5872(24) | 9323(19) | 9945(9) | 106(2) |
| C(33) | 8252(20) | 10345(20) | 9847(10) | 96(2) |
| C(41) | 6142(20) | 6192(15) | 8590(11) | 92(2) |
| C(42) | 6483(24) | 6190(16) | 9443(7) | 84(2) |
| C(43) | 8638(22) | 5900(18) | 8909(8) | 83(2) |
| C(1A) | 2266(17) | 2751(13) | 8202(5) | 38(2) |
| C(2A) | 1009(17) | 2963(15) | 8028(8) | 53(2) |
| C(3A) | 413(20) | 2365(18) | 7705(8) | 69(2) |
| C(4A) | 1047(20) | 1446(19) | 7579(7) | 70(2) |
| C(5A) | 2277(21) | 1193(14) | 7738(7) | 59(2) |
| C(6A) | 2810(20) | 1819(13) | 8066(7) | 56(2) |
| C(7A) | 2189(17) | 3039(12) | 9051(6) | 44(2) |
| C(8A) | 2687(19) | 2231(14) | 9278(6) | 49(2) |
| C(9A) | 2064(21) | 1803(17) | 9624(7) | 71(2) |
| C(10A) | 879(20) | 2219(17) | 9767(7) | 65(2) |
| C(11A) | 364(21) | 2984(17) | 9533(6) | 63(2) |
| C(12A) | 959(14) | 3419(17) | 9180(5) | 43(2) |
| C(13A) | 2642(16) | 4655(13) | 8511(7) | 52(2) |
| C(14A) | 2583(18) | 5334(13) | 8833(7) | 49(2) |
| C(15A) | 2457(20) | 6398(15) | 8781(7) | 65(2) |
| C(16A) | 2390(19) | 6766(13) | 8360(9) | 67(2) |
| C(17A) | 2467(20) | 6122(13) | 8032(6) | 52(2) |
| C(18A) | 2594(23) | 5090(15) | 8091(6) | 64(2) |
| C(19A) | 4566(15) | 3350(13) | 8607(5) | 34(2) |
| C(20A) | 5343(19) | 3233(16) | 8233(7) | 57(2) |
| C(21A) | 6701(18) | 3213(18) | 8245(8) | 68(2) |
| C(22A) | 7395(18) | 3244(14) | 8621(9) | 70(2) |
| C(23A) | 6689(15) | 3413(14) | 9009(7) | 48(2) |
| C(24A) | 5259(15) | 3446(15) | 9013(7) | 49(2) |
| B(1) | 2907(15) | 3439(16) | 8578(6) | 36(2) |

^a Equivalent isotropic *U* defined as one-third of the trace of the orthogonalized U_{ij} tensor.

(a doublet) and DD (a singlet) isotopomers. The triplet proton resonance due to the HD ligand is found superimposed on the broad line of the H_2 isotopomer. The NMR spectrum presented in Figure 1 and other ones of 2 measured at different temperatures do not give evidence for a resonance of a dihydride tautomer. Formation of the latter could be expected from related work. A complex $\text{Re}(\text{H}_2)(\text{CO})_2(\text{PMe}_2\text{Ph})_3^+$ was reported to exist in equilibrium with the classical dihydride tautomer in solution.^{2c}

The X-ray structure of the monohydride $\text{ReH}(\text{CO})_2(\text{PMe}_3)_3$ was determined. It crystallizes in the space group $P2_12_12_1$. There are two independent molecules in the unit cell. The coordination polyhedra can be described in both molecules as a distorted octahedron in which the three meridionally arranged PMe_3 ligands are noticeably bent toward the metal bound hydrogen atom (Figure 2; Table V). The angles between the trans PMe_3 ligands are equal to $160.1(3)$ and $168.1(3)^\circ$ in the two independent molecules A and B, respectively. The two trans phosphines show approximately equal Re–P bond lengths (2.377(8) and 2.389(9) Å), while the third Re–P bond is longer, 2.440(8) and 2.426(8) Å in molecules A and B, respectively. The hydride, two CO and the P(3) Me_3 ligands, and the rhenium atom form an approximate plane. There is some deviation (0.75(9) and 0.54(9) Å, in molecules A and B, respectively) of the hydride (to P(3) and P(6) atoms in molecules A and B, respectively) from the plane being

Table IV. Atomic Coordinates ($\times 10^4$) and Equivalent Isotropic Displacement Coefficients ($\text{\AA}^2 \times 10^3$) for $\text{ReH}_3(\text{CO})(\text{PMe}_3)_3$

| | x | y | z | $U(\text{eq})^a$ |
|-------|-----------|-----------|-----------|------------------|
| Re(1) | 2272(1) | 1897(1) | 0 | 40(1) |
| Re(2) | -514(1) | -2237(1) | 10(2) | 46(1) |
| P(1) | 2755(5) | 806(7) | 1185(6) | 47(1) |
| P(2) | 2716(4) | 742(8) | -1130(6) | 49(1) |
| P(3) | 1229(3) | 2281(4) | 483(4) | 40(1) |
| P(4) | 449(3) | -2884(4) | 830(4) | 45(1) |
| P(5) | -1203(2) | -554(3) | -51(8) | 38(1) |
| P(6) | -77(3) | -2198(5) | -1359(4) | 50(1) |
| O(1) | 1886(8) | 3681(13) | -1537(11) | 76(2) |
| O(2) | -1205(10) | -2643(15) | 1825(13) | 96(2) |
| C(1) | 2073(10) | 2981(15) | -1033(15) | 57(2) |
| C(2) | -928(13) | -2488(16) | 1131(17) | 75(2) |
| C(11) | 2442(14) | 887(22) | 2191(18) | 115(2) |
| C(12) | 2453(12) | -529(16) | 1377(17) | 79(2) |
| C(13) | 3601(10) | 721(15) | 1150(15) | 49(2) |
| C(21) | 2660(11) | 1598(18) | -2240(16) | 69(2) |
| C(22) | 2634(11) | -914(17) | -1121(16) | 73(2) |
| C(23) | 3640(14) | 507(21) | -1326(20) | 96(2) |
| C(31) | 585(10) | 2319(16) | -303(15) | 73(2) |
| C(32) | 1158(12) | 3615(15) | 1067(14) | 65(2) |
| C(33) | 873(10) | 1195(14) | 1231(14) | 56(2) |
| C(41) | 490(11) | -4455(17) | 1128(18) | 94(2) |
| C(42) | 570(11) | -2140(19) | 1829(16) | 75(2) |
| C(43) | 1277(12) | -2727(18) | 329(16) | 82(2) |
| C(51) | -1106(13) | 616(18) | -971(18) | 80(2) |
| C(52) | -2071(7) | -809(13) | -12(24) | 64(2) |
| C(53) | -1161(12) | 347(14) | 865(16) | 58(2) |
| C(61) | -670(12) | -2120(15) | -2244(14) | 63(2) |
| C(62) | 313(12) | -3575(19) | -1665(17) | 92(2) |
| C(63) | 514(10) | -1068(17) | -1679(15) | 74(2) |
| H(1) | 2955(30) | 2610(31) | -399(31) | 53(3) |
| H(2) | 2608(30) | 2382(31) | 933(31) | 51(3) |
| H(3) | 1752(29) | 667(31) | -65(32) | 54(3) |
| H(4) | -1155(30) | -2876(31) | -547(31) | 49(3) |
| H(5) | -348(29) | -3525(31) | 180(31) | 51(3) |
| H(6) | -58(29) | -1181(31) | 192(31) | 51(3) |

^a Equivalent isotropic U defined as one-third of the trace of the orthogonalized U_{ij} tensor.

Table V. Selected Bond Distances (\AA) and Angles (deg) for $\text{ReH}(\text{CO})_2(\text{PMe}_3)_3$

| molecule A | | molecule B | |
|-----------------|-----------|-----------------|----------|
| Re(1)-P(1) | 2.382(8) | Re(2)-P(4) | 2.389(9) |
| Re(1)-P(2) | 2.377(8) | Re(2)-P(5) | 2.381(8) |
| Re(1)-P(3) | 2.440(8) | Re(2)-P(6) | 2.426(8) |
| Re(1)-C(1) | 1.98(3) | Re(2)-C(3) | 1.86(3) |
| Re(1)-C(2) | 1.84(3) | Re(2)-C(4) | 1.96(3) |
| Re(1)-H(1) | 1.98(8) | Re(2)-H(2) | 1.99(8) |
| C(1)-O(1) | 1.12(4) | C(3)-O(3) | 1.20(4) |
| C(2)-O(2) | 1.19(4) | C(4)-O(4) | 1.16(4) |
| P(1)-Re(1)-P(2) | 160.1(3) | P(4)-Re(2)-P(5) | 168.1(3) |
| P(1)-Re(1)-P(3) | 92.4(3) | P(4)-Re(2)-P(6) | 94.0(3) |
| P(2)-Re(1)-P(3) | 91.8(3) | P(5)-Re(2)-P(6) | 92.4(3) |
| P(1)-Re(1)-C(1) | 99.1(9) | P(4)-Re(2)-C(3) | 85.7(10) |
| P(2)-Re(1)-C(1) | 100.5(9) | P(5)-Re(2)-C(3) | 86.6(10) |
| P(3)-Re(1)-C(1) | 87.6(9) | P(6)-Re(2)-C(3) | 173.0(9) |
| P(1)-Re(1)-C(2) | 89.7(10) | P(4)-Re(2)-C(4) | 94.1(9) |
| P(2)-Re(1)-C(2) | 87.4(11) | P(5)-Re(2)-C(4) | 95.5(9) |
| P(3)-Re(1)-C(2) | 175.8(12) | P(6)-Re(2)-C(4) | 92.9(8) |
| C(1)-Re(1)-C(2) | 88.4(14) | C(3)-Re(2)-C(4) | 94.1(12) |
| P(1)-Re(1)-H(1) | 84(3) | P(4)-Re(2)-H(2) | 80(2) |
| P(2)-Re(1)-H(1) | 78(3) | P(5)-Re(2)-H(2) | 92(2) |
| P(3)-Re(1)-H(1) | 73(2) | P(6)-Re(2)-H(2) | 77(2) |
| C(1)-Re(1)-H(1) | 160(3) | C(3)-Re(2)-H(2) | 96(2) |
| C(2)-Re(1)-H(1) | 111(3) | C(4)-Re(2)-H(2) | 167(3) |

orthogonal to the previous one in which the metal, axial phosphanes, and the carbon atom of one CO ligand lie.

When $\text{ReH}(\text{CO})_2(\text{PMe}_3)_3$ is protonated, its basic solution structure is obviously only marginally perturbed. For **1** a geometry similar to that of the isoelectronic Kubas complex $\text{W}(\text{H}_2)(\text{CO})_3(\text{PPr}^i)_3$ can be expected. The suggested structures for **1** and **2** are depicted in Chart I.

Table VI. Selected Bond Distances (\AA) and Angles (deg) for $[\text{ReH}_2(\text{CO})(\text{PMe}_3)_4][\text{BPh}_4]$

| | | | |
|-----------------|----------|-----------------|----------|
| Re(1)-P(1) | 2.448(6) | C(1)-O(1) | 1.24(3) |
| Re(1)-P(2) | 2.449(6) | B(1)-C(1A) | 1.61(3) |
| Re(1)-P(3) | 2.440(6) | B(1)-C(7A) | 1.71(3) |
| Re(1)-P(4) | 2.361(4) | B(1)-C(13A) | 1.64(3) |
| Re(1)-C(1) | 1.81(3) | B(1)-C(19A) | 1.67(2) |
| Re(1)-H(1) | 1.74(7) | | |
| Re(1)-H(2) | 1.84(5) | | |
| P(1)-Re(1)-P(2) | 91.3(2) | P(1)-Re(1)-P(3) | 91.6(2) |
| P(2)-Re(1)-P(3) | 95.3(2) | P(1)-Re(1)-P(4) | 132.7(2) |
| P(2)-Re(1)-P(4) | 99.4(2) | P(3)-Re(1)-P(4) | 132.4(2) |
| P(1)-Re(1)-C(1) | 91.2(8) | P(2)-Re(1)-C(1) | 177.5(8) |
| P(3)-Re(1)-C(1) | 84.7(8) | P(4)-Re(1)-C(1) | 78.8(7) |
| P(1)-Re(1)-H(1) | 56(1) | P(2)-Re(1)-H(1) | 94(3) |
| P(3)-Re(1)-H(1) | 147(2) | P(4)-Re(1)-H(1) | 77.2(2) |
| C(1)-Re(1)-H(1) | 87(3) | P(1)-Re(1)-H(2) | 153(1) |
| P(2)-Re(1)-H(2) | 81(3) | P(3)-Re(1)-H(2) | 64(2) |
| P(4)-Re(1)-H(2) | 75(2) | C(1)-Re(1)-H(2) | 97(3) |

Table VII. Selected Bond Distances (\AA) and Angles (deg) for $\text{ReH}_3(\text{CO})(\text{PMe}_3)_3$

| molecule A | | molecule B | |
|-----------------|-----------|-----------------|-----------|
| Re(1)-P(1) | 2.427(9) | Re(2)-P(4) | 2.454(6) |
| Re(1)-P(2) | 2.372(9) | Re(2)-P(5) | 2.391(4) |
| Re(1)-P(3) | 2.299(6) | Re(2)-P(6) | 2.296(7) |
| Re(1)-C(1) | 2.063(21) | Re(2)-C(2) | 1.948(26) |
| Re(1)-H(1) | 1.73(5) | Re(2)-H(4) | 1.73(6) |
| Re(1)-H(2) | 1.69(5) | Re(2)-H(5) | 1.54(4) |
| Re(1)-H(3) | 1.77(5) | Re(2)-H(6) | 1.56(5) |
| P(1)-Re(1)-P(2) | 96.3(3) | P(4)-Re(2)-P(5) | 137.4(3) |
| P(1)-Re(1)-P(3) | 103.3(3) | P(4)-Re(2)-P(6) | 99.8(2) |
| P(2)-Re(1)-P(3) | 134.4(2) | P(5)-Re(2)-P(6) | 100.2(3) |
| P(1)-Re(1)-C(1) | 166.9(6) | P(4)-Re(2)-C(2) | 81.0(8) |
| P(2)-Re(1)-C(1) | 81.0(6) | P(5)-Re(2)-C(2) | 84.3(7) |
| P(3)-Re(1)-C(1) | 87.3(6) | P(6)-Re(2)-C(2) | 172.0(6) |
| H(1)-Re(1)-H(2) | 80(3) | H(4)-Re(2)-H(5) | 81(2) |
| H(1)-Re(1)-H(3) | 147(2) | H(4)-Re(2)-H(6) | 151(2) |
| H(2)-Re(1)-H(3) | 124(2) | H(5)-Re(2)-H(6) | 126(3) |

On warming of **1** and **2** in solution, they decompose with irreversible evolution of H_2 . **1** turned out to be especially unstable. It slowly transforms into some non-hydride products even at -95°C (^{31}P NMR detection). **2** is stable in solution at temperatures below -55 to -50°C .

Preparation and Characterization of $\text{Re}(\text{H}_2)(\text{CO})(\text{PMe}_3)_4^+$ (3a**) and $\text{Re}(\text{H})_2(\text{CO})(\text{PMe}_3)_4^+$ (**3b**).** The reaction of the mono hydride *cis*- $\text{ReH}(\text{CO})(\text{PMe}_3)_4$ with CF_3COOH in dichloromethane at -95°C affords the molecular hydrogen complex $\text{Re}(\text{H}_2)(\text{CO})(\text{PMe}_3)_4^+$ (**3a**). The ^1H NMR spectrum of **3a** shows a broad signal at $\delta -6.45$ with a short $T_{1\text{min}}$ value of 9 ms (at 183 K), characteristic of a dihydrogen ligand. *cis*- $\text{ReH}(\text{CO})(\text{PMe}_3)_4$ forms a mixture of isotopomers of **3a** upon protonation with CF_3COOD . Similarly to the spectra of **2** presented in Figure 1, the ^1H and ^2H NMR spectra of partially deuterated **3a** (Figure 3) reveal a large J_{HD} coupling of 27.7 Hz. However, the ^1H NMR spectrum also contains remarkably well-resolved $^2J_{\text{HP}}$ couplings of 9.4 and 4.7 Hz; i.e., each component of the H-D triplet is additionally split into a doublet of quartets. The whole spectrum is consistent with an octahedral structure of **3a** with one of the phosphorus atoms trans to the HD moiety (Chart II). **3a** is very likely the kinetic product of the protonation, retaining the structure of the starting compound *cis*- $\text{ReH}(\text{CO})(\text{PMe}_3)_4$.

A trans phosphorus donor ligand is expected to enhance back-donation to a coordinated H_2 ,⁴ generating preference for a dihydride structure. In accordance with this simple consideration **3a**, being prepared at -95°C , irreversibly transforms into ReH_2 -

- (3) Kubas, G. J.; Unkefer, C. J.; Swanson, B. I.; Fukushima, E. *J. Am. Chem. Soc.* **1986**, *108*, 7000.
- (4) Burdett, J. K.; Eisenstein, O.; Jackson, S. A. In *Transition Metal Hydrides*; Dedieu, A., Ed.; VCH Publishers, Inc.: Deerfield Beach, FL 1992; Chapter 5.

Table VIII. ^1H NMR Spectroscopic Data for Complexes 1–5

| complex | ReH_n | | $\text{Re}(\text{H}_2)$ | | |
|---|----------------|------------------------|-------------------------|------------------------|----------------------|
| | δ , ppm | $T_{1\text{min}}$, ms | δ , ppm | $T_{1\text{min}}$, ms | $J(\text{H-D})$, Hz |
| $\text{Re}(\text{H}_2)(\text{CO})_3(\text{PMe}_3)_2^+$ (1) | | | -4.70 | 6.7 | 33 ^a |
| $\text{Re}(\text{H}_2)(\text{CO})_2(\text{PMe}_3)_3^+$ (2) | | | -4.73 | 8.2 | 33.7 |
| $\text{Re}(\text{H}_2)(\text{CO})(\text{PMe}_3)_4^+$ (3a) | | | -6.45 | 9.0 | 27.7 |
| $\text{ReH}_2(\text{CO})(\text{PMe}_3)_4^+$ (3b) | -5.89 | 210 | | | |
| $\text{Re}(\text{H})_2(\text{H}_2)(\text{CO})(\text{PMe}_3)_3^+$ (4a) | -5.53 | 115 | -6.0 | 8.3 | 33.6 |
| $\text{ReH}_4(\text{CO})(\text{PMe}_3)_3^+$ (4b) | -4.79 | 130 | | | |
| $\text{ReH}(\text{H}_2)(\text{CO})(\text{NO})(\text{PPr}_3)_2^+$ (5) | -2.46 | 68 ^b | -2.0 | 7.3 ^c | <i>d</i> |

^a This value may be underestimated because of substantial broadening of the H-D triplet. ^b This value obtained at the lowest attainable temperature (158 K) could be underestimated due to an exchange between the classical and nonclassical sites in 5. ^c $T_{1\text{min}}$ time measured for the averaged resonance because of a fast exchange between the hydride and dihydrogen ligands in 5 at 193 K. Assuming that $1/T_{1\text{min}}(\text{H}_2) \gg 1/T_{1\text{min}}(\text{H})$, a relaxation time of 4.9 ms can be calculated for $T_{1\text{min}}(\text{H}_2)$. ^d A broad resonance due to the presence of an H-D ligand was observed in the low-temperature ^1H NMR spectra of partially deuterated 5.

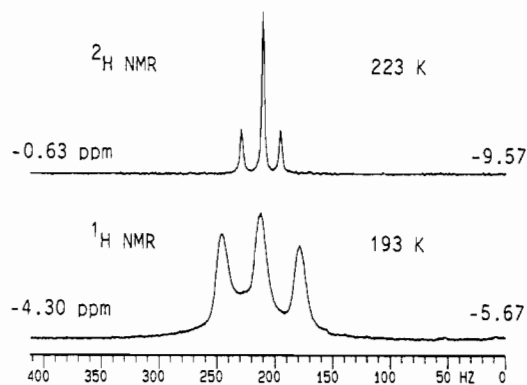


Figure 1. H_2 , HD, and D_2 resonances in the ^1H and ^2H NMR spectra of an isotopomeric mixture of 2.

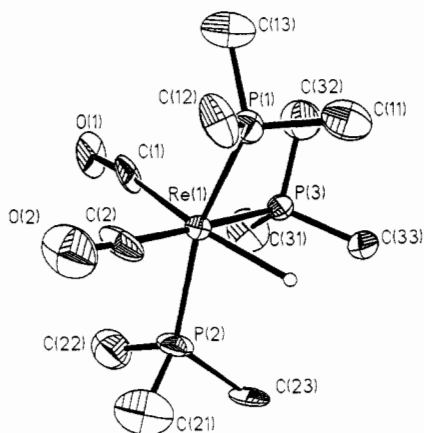
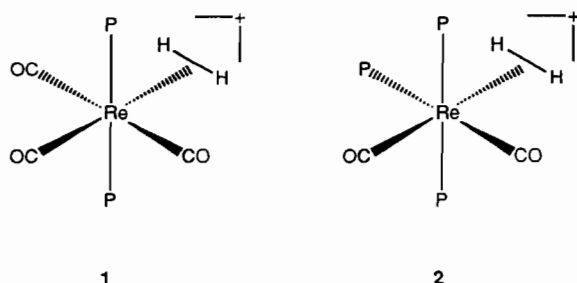


Figure 2. Molecular structure of one of the two independent molecules of $\text{ReH}(\text{CO})_2(\text{PMe}_3)_3$. Thermal ellipsoids are drawn at the 50% probability level.

Chart I



$(\text{CO})(\text{PMe}_3)_4^+$ (3b) in solution at temperatures above -30°C . This dihydride has been previously obtained by protonation of $\text{Re}(\text{CO})(\text{O}_2\text{CH})(\text{PMe}_3)_4$ with HBF_4 in diethyl ether,⁵ and the related complex $\text{ReH}_2(\text{CO})(\text{PMe}_2\text{Ph})_4^+$ has been prepared by protonation of $\text{ReH}(\text{CO})(\text{PMe}_2\text{Ph})_4$ with $\text{HBF}_4 \cdot \text{OME}_2$ in CH_2 -

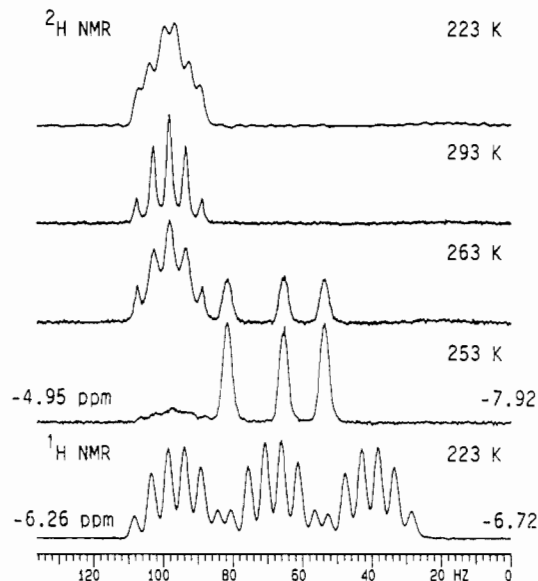
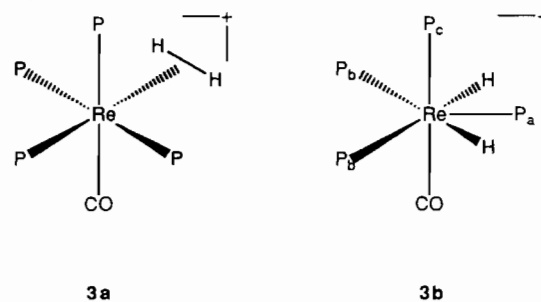


Figure 3. ^1H and temperature-dependent ^2H NMR spectra (hydride region) of an isotopomeric mixture resulting from the reaction between *cis*- $\text{ReH}(\text{CO})(\text{PMe}_3)_4$ and CF_3COOD . The ^1H NMR spectrum was obtained by the inversion-recovery method ($180^\circ - \tau - 90^\circ$) with the delay time τ short enough to null the resonance due to the coordinated H_2 in 3a.

Chart II



Cl_2 at 25°C .^{2c} It should be noted that, in both cases, a *trans* $\text{H}(\text{O}_2\text{CH})$, CO geometry has been claimed for the starting complexes from their room-temperature NMR data. On the basis of our experience, we believe that the reported observations of singlet resonances in the ^{31}P NMR spectra of $\text{Re}(\text{CO})(\text{O}_2\text{CH})(\text{PMe}_3)_4$ and $\text{ReH}(\text{CO})(\text{PMe}_2\text{Ph})_4$ indicate rapid fluxionality at room temperature, which precludes any structural assignments.

The transformation of 3a into 3b is demonstrated by the ^2H NMR spectra presented in Figure 3. ReDH and ReD_2 resonances of 3b of low intensity are observed at 253 K at $\delta -5.9$, and the

(5) Allen, D. L.; Green, M. L. H.; Bandy, J. A. *J. Chem. Soc., Dalton Trans.* 1990, 541.

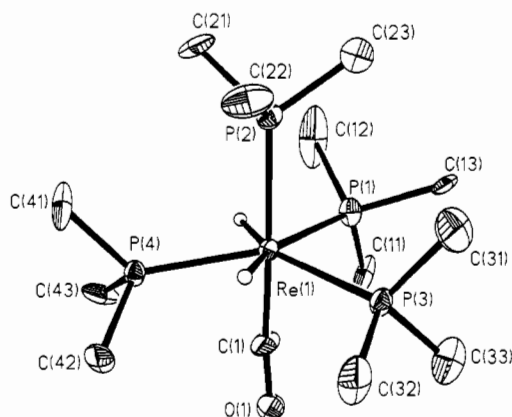


Figure 4. Molecular structure of $\text{ReH}_2(\text{CO})(\text{PMe}_3)_4^+$. Thermal ellipsoids are drawn at the 50% probability level.

intensity strongly increases by warming the solution by 10° . At 293 K the signal appears as a well-resolved quintet ($^2J_{\text{DP}} = 4.9$ Hz) because of a fast intramolecular ligand exchange leading to an averaging of the deuterium–phosphorus couplings. In addition in the room-temperature ^1H NMR spectrum of **3b** a quintet ($^2J_{\text{HP}} = 32$ Hz) with broadened three inner lines has been observed.

On lowering of the temperature, the ligand exchange becomes slow, and at 200 K, the ^1H and ^{31}P NMR spectra of **3b** are interpreted in terms of an $\text{AA}'\text{XYZZ}'$ (A, A' , ^1H ; $\text{X}, \text{Y}, \text{Z}, \text{Z}'$, ^{31}P) spin system.

The X-ray structure of $[\text{ReH}_2(\text{CO})(\text{PMe}_3)_4]\text{BPh}_4^-$ reveals well-separated ions. The anion BPh_4^- displays expected tetrahedral geometry. For the cation $\text{ReH}_2(\text{CO})(\text{PMe}_3)_4^+$ the coordination polyhedron is a distorted pentagonal bipyramid with CO and PMe_3 ligands in the axial positions (Figure 4; Table VI). The $\text{OC}-\text{Re}-\text{PMe}_3$ fragment being practically linear ($177.5(8)^\circ$) is orthogonal (93.0°) to the plane containing P(1), Re, P(3), H(1), and H(2) atoms. For P(4) there is a small deviation from this plane (by 0.67 \AA), forming equal angles ($132.7(2)$ and $132.4(2)^\circ$) to P(1) and P(3). The two H ligands occupy positions between P(4) and P(1), and P(4) and P(3).

The solid-state structure is presumably retained in solution allowing clarification of the low-temperature NMR data. For an $\text{AA}'\text{XYZZ}'$ spin system the XY part of P_a and P_c (this and the following assignments are in accordance with the notations used in Chart II) represents first-order multiplets, while the AA' (the H-ligands) and ZZ' (2P_b) parts are complex non-first-order patterns with the separation between the outermost intense lines being the sums: $J_{\text{AX}} + J_{\text{AY}} + J_{\text{AZ}} + J_{\text{AZ}'}$ and $J_{\text{ZA}} + J_{\text{ZA}'} + J_{\text{ZX}} + J_{\text{ZY}}$, respectively.⁶ The constants are extracted via simulation of the low-temperature spectrum of **3b** and are listed in the Experimental Section; the most important of them are the couplings between the cis H and P_c of 20.7 Hz and the large A–X, A'–X (44.7 Hz) and A–Z, A'–Z' (54 Hz) couplings between the hydrides and the phosphorus nuclei (P_a and P_b) in the plane.

A comparison of the X-ray structure of **3b** and the structure of **3a** based on the NMR data allows us to conclude that formation of the thermodynamically favorable **3b** may result from scission of the H–H bond in **3a** followed by a migration of one H through a P–Re–CO plane without significant topological perturbation of the residual coordination sphere.

Preparation and Characterization of $\text{Re}(\text{H}_2)(\text{H})_2(\text{CO})(\text{PMe}_3)_3^+$ (4a**) and $\text{ReH}_4(\text{CO})(\text{PMe}_3)_3^+$ (**4b**).** Protonation of $\text{ReH}_3(\text{CO})(\text{PMe}_3)_3$ with CF_3COOH in dichloromethane at -95°C leads to an equilibrium mixture of the tautomers, $\text{Re}(\text{H}_2)(\text{H})_2(\text{CO})(\text{PMe}_3)_3^+$ (**4a**) and $\text{ReH}_4(\text{CO})(\text{PMe}_3)_3^+$ (**4b**). Figure 5 shows the low-temperature ^1H NMR spectrum of **4a,b** together

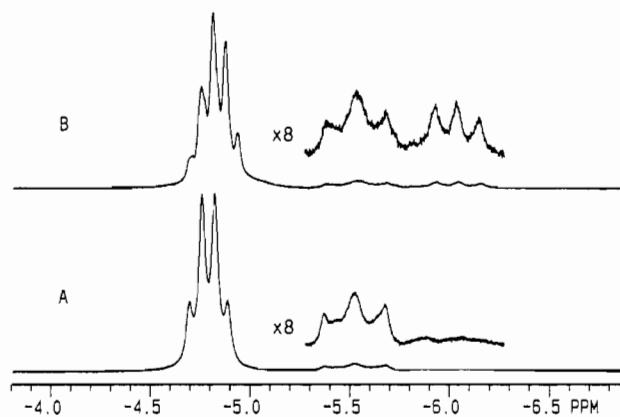


Figure 5. Hydride region of the ^1H NMR spectra of **4** (A) and of a mixture of isotopomers of the deuterated complex **4** (deuterium content $< 75\%$) at 168 K (B).

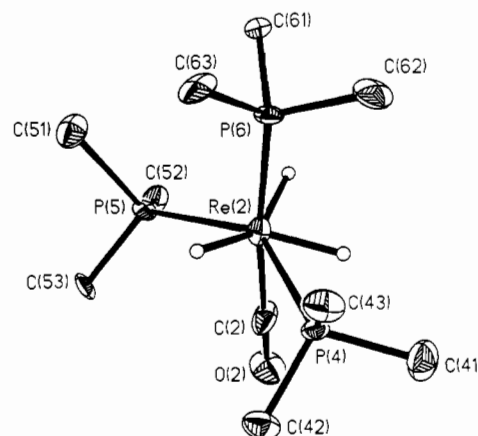


Figure 6. Molecular structure of one of the two independent molecules of $\text{ReH}_3(\text{CO})(\text{PMe}_3)_3$. Thermal ellipsoids are drawn at the 50% probability level.

with the spectrum of a mixture of isotopomers formed when $\text{ReD}_3(\text{CO})(\text{PMe}_3)_3$ was protonated with CF_3COOH . The formation of an isotopomeric mixture in the latter case is clearly supported by the appearance of distortions in the resonance at $\delta -4.82$ of partially deuterated **4b** (Figure 5A) as a result of an overlapping of quartet resonances. The H–D ligand resonance of **4a** is observed as a triplet ($J_{\text{HD}} = 33.6$ Hz) at $\delta -6.04$.

An inspection of the spectra presented in Figure 5 and those reported previously for a mixture of $\text{Re}(\text{H}_2)(\text{H})_2(\text{CO})(\text{PMe}_2\text{Ph})_3^+$ (**4a'**) and $\text{ReH}_4(\text{CO})(\text{PMe}_2\text{Ph})_3^+$ (**4b'**)^{2a,b} allows one to conclude that protonation of $\text{ReH}_3(\text{CO})(\text{PMe}_3)_3$ gives a system being very similar to that formed by protonation of $\text{ReH}_3(\text{CO})(\text{PMe}_2\text{Ph})_3$.

According to the X-ray data, both independent molecules of $\text{ReH}_3(\text{CO})(\text{PMe}_3)_3$ contain Re(III) atoms with the unusual coordination number of 7. Formally the ligand polyhedra in each molecule are close to pentagonal bipyramids with PMe_3 and CO ligands in the axial positions (Figure 6; Table VII). The same geometry was found for $\text{ReH}_3(\text{PMePh}_2)_4$ with an average Re–H distance of 1.76 \AA and almost equal Re–P bonds (2.354 – 2.388 \AA).⁷ The structure of $\text{ReH}_3(\text{PMe}_3)_3\text{CO}$ resembles that of $\text{ReH}_2(\text{CO})(\text{PMe}_3)_4^+$; the former is related to the latter by formal replacement of an equatorial H ligand with PMe_3 . In both molecules of $\text{ReH}_3(\text{PMe}_3)_3\text{CO}$ one finds strongly differing Re–P bond lengths ($2.427(9)$ – $2.299(6) \text{ \AA}$ in molecule A and $2.454(6)$ – $2.296(7) \text{ \AA}$ in molecule B). However the average Re–H distances (1.73 and 1.61 \AA , in molecule A and B, respectively) are close to the values in $\text{ReH}_3(\text{PMePh}_2)_4$ ⁷ and in $\text{ReH}_5(\text{PMePh}_2)_3$

(6) (a) Jesson, J. P.; Muetterties, E. L.; Meakin, P. *J. Am. Chem. Soc.* **1971**, *93*, 5261. (b) Meakin, P.; Guggenberger, L. J.; Peet, W. G.; Muetterties, E. L.; Jesson, J. P. *J. Am. Chem. Soc.* **1973**, *95*, 1467.

(7) Cotton, F. A.; Luck, R. L. *Inorg. Chem.* **1989**, *28*, 2181.

(1.688(5) Å)⁸ and K₂ReH₉ (1.68(1) Å),⁹ which were determined by neutron diffraction.

There is a great resemblance of the couplings and relative chemical shifts in the low-temperature ¹H NMR spectra of the **4a** + **4b** and **4a'** + **4b'** mixtures. From the spectral features the most important point is the apparent triplet splitting of the Re-(H)₂ resonances of 46 and 55 Hz for **4b** (δ -5.53) and **4b'**, respectively. Neglecting the expectedly small couplings to the dihydrogen ligand, these resonances are assigned to the AA' part of an AA'XYY' (X, Y, Y', ³¹P) spin system with the splittings determined by the sum: $J_{AX} + J_{AY} + J_{AY'}$. Consequently, we can conclude that the molecular geometries of **4b** and **4b'** should not be appreciably different, since coupling constants would normally be strongly affected by structural changes.

The equilibrium constants for the conversion of **4b** to **4a** determined by integration of the respective resonances in the ¹H and ³¹P(¹H) NMR spectra (temperature range 163–223 K) provide a linear ln K_{eq} vs 1/T plot with the following thermodynamic parameters: Δ*H* = 1.05 ± 0.1 kcal/mol and Δ*S* = 2.3 ± 0.6 eu. For the conversion of **4b'** to **4a'** the values of Δ*H* of 1.1 ± 0.2 kcal/mol and Δ*S* of 2.4 ± 0.8 eu were determined,^{2b} which are well compared with those of the **4b** to **4a** transformation. In agreement with the observed isotope effect on the equilibrium between partially deuterated **4a'** and **4b'** the K_{eq} values for partially deuterated **4a** and **4b** are substantially greater than those for the perprotio complexes. At 183 K, for example, K_{eq}^H is equal to 0.16 and K_{eq}^D is equal to 0.24, which corresponds to ca. 0.15 kcal mol⁻¹ difference in Δ*H*_H and Δ*H*_D values.

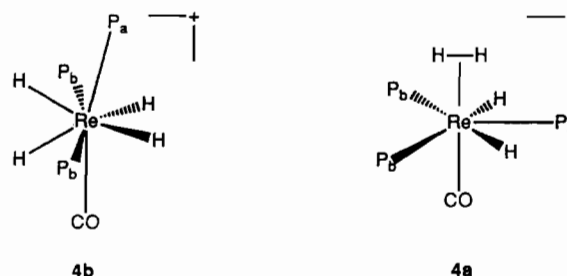
For the classical tautomer **4b** we assume a dodecahedral structure, which was also suggested previously^{2b} for **4b'**. This coordination geometry would be consistent with the observation of an AB₂ pattern (δ -41.5, -43.3; J_{PP} = 16.6 Hz) in the ³¹P NMR spectrum and a doublet of triplets (δ 193.8; $^2J_{CP}$ = 24.1, 5.6 Hz) for the CO ligand in the ¹³C(¹H) NMR spectrum of **4b**. The largest ¹³C-³¹P coupling constant is substantially less than those expected for CO trans to PMe₃, in agreement with the absence of real trans sites in an idealized dodecahedron.

An intramolecular pairwise exchange of the H ligands of **4b** represents a possible reorientation process which leads to averaging of the ReH₄ resonances of **4b** even at the lowest attainable temperature, 163 K. At the same time the "(CO)(PMe₃)₃ frame" of ReH₄(CO)(PMe₃)₃⁺ stays quite rigid. In the ¹³C NMR spectrum of **4b** measured at 183–203 K the CO resonance is well-resolved. There is considerable broadening of the AB₂ phosphorus pattern of **4b** at 233 K, although the lines are still well-separated (by 227 Hz). In the ¹H NMR spectrum at 233 K the quartet of the ReH₄ unit is also broadened, so that only the intense lines are resolved. In the temperature range 243–253 K the interconversion between **4b** and **4a**, which represents the real reason for the spectral changes described above, becomes fast enough to average the hydride NMR resonances of the tautomers.

Thus, a suggestion^{2b} of very low barriers based on the assumption of a rearrangement of the non-hydride ligands like in eight-coordinate complexes obviously does not hold in the present case. It would be also inconsistent with literature data. It is known that in the complexes of the type MH₄L₄, MH₄L₂L' (M = W, L = tertiary phosphane, L' = bidentate phosphane; M = Mo, L = tertiary phosphane) the rearrangement barriers are relatively high, Δ*G*[‡] = 12–16 kcal mol⁻¹.^{6b} The barriers have been found to be relatively insensitive to ligand variations, but they are definitely higher for heavier transition metal centers.

Under these circumstances it is quite surprising that the AB₂ pattern of Re(H₂)(H)₂(PMe₃)₃⁺ (δ -21.1, -39.8; $^2J_{PP}$ = 26 Hz) becomes strongly broadened in low-temperature ³¹P NMR spectra.

Chart III



The 26-Hz $^2J_{PP}$ coupling constant can be resolved only at temperatures below 183 K (note that the separation of the ³¹P resonances of **4a** is 10 times that observed for **4b**).

Simulation of the ³¹P NMR spectra of **4a** recorded in the temperature range 178–233 K with use of the DNMR4 program¹⁰ allowed an investigation of the rate of the exchange process averaging the ³¹P resonances of **4a**. An Eyring plot yielded the activation enthalpy and entropy, Δ*H*[‡] = 8.0 ± 0.2 kcal/mol and Δ*S*[‡] = -3.7 ± 1 eu, respectively (Figure 7). Remarkably, a simulation of the ³¹P NMR spectra of partially deuterated **4a** (deuterium content < 75%), recorded in the same temperature range, revealed a pronounced isotope effect on the rate of the dynamic process (Δ*H*[‡] = 8.6 ± 0.2 kcal/mol, Δ*S*[‡] = -1.7 ± 1 eu; k_H/k_D = 2 at 183 K). This observation suggests H-H (H-D, D-D) bond cleavage as a rate-determining step. At the same time the small values of Δ*S*[‡] are consistent with an intramolecular mechanism for the process.

In the ¹H NMR spectra the Re(H)₂ and Re(H₂) resonances of **4a** coalesce at 185 K and the line width of the resulting signal observed is 230 Hz at this temperature. Assuming a two-site exchange and using the well-known equation¹¹ $k = \pi\Delta\nu/\sqrt{2}$ to calculate the rate constant for the coalescence temperature, a very rough estimate of k of 313 s⁻¹ (Δ*G*[‡] = 8.5 kcal mol⁻¹) can be obtained by applying the experimental value for Δ*ν* of 141 Hz. This rate constant is doubtlessly overestimated because of neglecting factors which usually influence a spectrum at a coalescence temperature: spin-spin relaxation rate (1/*T*₂) and coupling constants.¹¹ In the present case they are especially important, being comparable to the Δ*ν* value. Thus, a more reasonable estimate for k at 185 K is the value of 230–240 s⁻¹ (Δ*G*[‡] = 8.6 kcal mol⁻¹), which we have obtained with *T*₂ = 4–5 ms and simulation of the observed ¹H NMR spectrum using the DNMR4 program.¹⁰ At 185 K the activation parameters calculated from the variable-temperature ³¹P NMR spectra amount to Δ*G*[‡] = 8.7 kcal mol⁻¹ and k = 226 s⁻¹ for the process averaging the AB₂ pattern of **4a**. Thus, this result substantiates the idea that exchange between the hydride and dihydrogen ligands also involves some distortion of the phosphorus ligand framework, however, without polytopal rearrangement of it.

The most reasonable structure for **4a**, explaining the intramolecular dynamic process, is surprisingly similar to the X-ray structure of ReH₂(CO)(PMe₃)₄⁺ (Chart III). This molecular geometry of **4a** is also strongly supported by the low-temperature NMR data. The observation of a quartet CO resonance (δ 194.2) at 178 K with a coupling constant $^2J_{CP}$ of 9 Hz is typical of a CO group located cis to three phosphane ligands. Another structurally relevant result is provided by the analysis of the hydride-coupled ³¹P NMR spectrum of **4a** recorded at the slow-exchange limit of 163 K. Neglecting the expectedly small couplings to the H₂ protons, this spectrum represents the XYY' part of an AA'XYY' spin system. All coupling constants obtained by simulation of

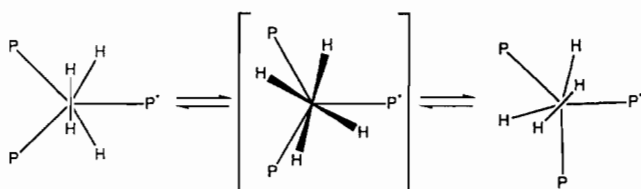
(8) Emge, T. J.; Koetzle, T. F.; Bruno, J. W.; Caulton, K. G. *Inorg. Chem.* **1984**, *23*, 4012.

(9) Abrahams, S. C.; Ginsberg, A. P.; Knox, K. *Inorg. Chem.* **1964**, *3*, 558.

(10) Bushweller, C. H.; Letenare, L. J.; Brunelle, J. A.; Bilofsky, H. S.; Whalon, M. R.; Fleischman, S. H. Quantum Chemistry Program Exchange, No. 466, DNMR-4.

(11) Oki, M. In *Methods in Spectrochemical Analysis*; Marchand, A. P., Ed.; VCH Publishers, Inc.: Deerfield Beach, FL, 1985; Chapter 1.

Chart IV



the spectrum are listed in the Experimental Section. Some of them are presented here. They amount to large absolute values of $J_{AX} = 44$ Hz and $J_{AY} = 47$ Hz between the hydrides and the phosphorus nuclei (P_a , P_b , and P_b' , Chart III), strongly suggestive of the absence of a cis arrangement of the hydride and phosphane ligands. Having compared the whole set of the ^{31}P chemical shifts and coupling constants of **3b** and **4a**, we find an extremely close resemblance of the $P_aP_bP_b'$ HH' spin systems in **3b** and **4a** (Charts II and III). We therefore believe that both molecules are very similar in geometry.

An intramolecular mechanism is proposed for the dynamic process in **4a**, which involves H–H bond cleavage followed by formation of a symmetric transition state presented in Chart IV. In this case a return to the ground-state dihydrogen complex will generate a new configuration of the in-plane ligands simulating an “exchange” of the chemically inequivalent phosphanes. We believe that a free energy of activation for the isomerization of **4a** \rightarrow **4b** taking place among the non-hydride ligands should be similar to that found for rearrangement processes of MH_4L_4 , MH_4L_2 complexes,^{6b} i.e. at least 3–4 kcal mol⁻¹ higher than the barrier for the intramolecular exchange between the hydride and dihydrogen ligands in **4a**. This would be in agreement with the ΔG^\ddagger value of 12.6 ± 0.2 kcal mol⁻¹ estimated for the conversion of **4a'** to **4b'**.^{2b}

Thus, the mechanism of the exchange between (H)₂ and (H₂) ligands suggested in this work for $\text{Re}(\text{H}_2)(\text{H})_2(\text{CO})(\text{PMe}_2)_3^+$ differs from that proposed by Luo and Crabtree for $\text{Re}(\text{H}_2)(\text{H})_2(\text{CO})(\text{PMe}_2\text{Ph})_3^+$, the latter involving formation of an $\eta^3\text{-H}_3$ complex, $[\text{ReH}(\eta^3\text{-H}_3)(\text{CO})(\text{PMe}_2\text{Ph})_3]^+$, as an intermediate or transition state.^{2b} It should be noted that our data do not rule out the possibility of formation of such an unstable intermediate or transient. However, out of these two models ours assuming an H–H bond breakage seems to provide the simplest explanation for the given kinetic data. The Luo and Crabtree model which implies formation of a new bond in the transition state (or intermediate) is an unlikely one. The only argument in support of the “trihydrogen” model is based on the evaluation of the rearrangement barrier in eight-coordinate complexes which is estimated to be “very low”. Following this consideration, formation of an eight-coordinate transition state cannot be a mechanism of the hydride–dihydrogen exchange, if it is much faster than the interconversion of the tautomers. In light of the available experimental data this argument is speculative, and in the absence of additional supporting experimental data a mechanism assuming rupture of the H–H ligand bond has to be favored.

Preparation and Characterization of $\text{ReH}(\text{H}_2)(\text{CO})(\text{NO})(\text{PPr}^i_3)_2^+$ (5**).** The reaction of the dihydride *cis*- $\text{ReH}_2(\text{CO})(\text{NO})(\text{PPr}^i_3)_2$ ¹² with an excess of CF_3COOH in dichloromethane leads to evolution of a broad resonance ($\delta -2.1$) in the hydride region of the ^1H NMR spectrum at 193 K. On lowering of the temperature, it decoalesces into two lines. While one of these becomes a well-resolved triplet ($\delta -2.46$, $^2J_{\text{HP}} = 24.4$ Hz) attributable to an H ligand, the other one broadens strongly and even “disappears” at the lowest attainable temperature of 158 K (Figure 8). These observations together with a short $T_{1\text{min}}$ time of 7.3 ms found for the averaged resonance at 193 K indicate formation of a dihydrogen complex $\text{ReH}(\text{H}_2)(\text{CO})(\text{NO})(\text{PPr}^i_3)^+$ (**5**).

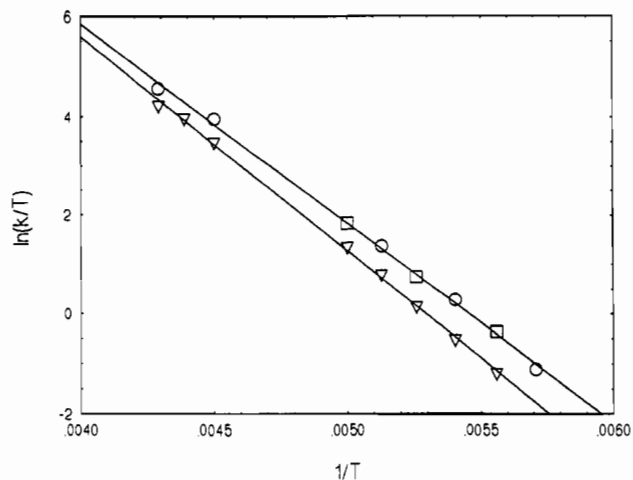


Figure 7. $\ln(k/T)$ vs $1/T$ dependencies (Eyring plots) for the intramolecular exchange process leading to averaging of the phosphane resonances in the ^{31}P NMR spectra of **4b** (O, □; data obtained with two independently prepared samples) and an isotopomeric mixture of complex **4b** (▽; deuterium content < 75%). Key: O, □, $\Delta H^\ddagger = 8.0 \pm 0.2$ kcal/mol, $\Delta S^\ddagger = -3.7 \pm 1$ eu; ▽, $\Delta H^\ddagger = 8.6 \pm 0.2$ kcal/mol, $\Delta S^\ddagger = -1.7 \pm 1$ eu.

Freezing of the intramolecular exchange between the H and H₂ ligands in **5** at low temperature is qualitatively similar to that observed for **4a**. In the slow-exchange spectrum presented in Figure 5 the dihydrogen resonance is also extremely broad and difficult to detect because of fast spin–spin relaxation. Partial deuteration of a dihydrogen complex commonly makes this relaxation less efficient due to substantially weaker dipole–dipole interactions between deuterons and protons. The ^1H NMR spectra of the mixture of isotopomers of **5** (Figure 8) prepared by the reaction of $\text{ReH}_2(\text{CO})(\text{NO})(\text{PPr}^i_3)_2$ with an excess of CF_3COOD also show this effect. A resonance, which can be attributed to the HD ligand, is found at $\delta -1.91$ at a temperature (158 K) when the H₂ resonance of **5** is unobservable. At the same time the spectrum does not show the expected H–D coupling and the line width of the HD signal is less than 50 Hz at 158 K. A broader line could be expected, since the short $T_{1\text{min}}$ relaxation time measured for the averaged resonance indicates a short H–H bond. Generally a total width of the strongly broadened H–D triplet (with $J_{\text{HD}} > 30$ Hz) of more than 60 Hz can be expected in such a case.

A similar observation has recently been made at comparable temperatures for $\text{Ru}(\text{H})_2(\text{H}_2)(\text{CO})(\text{PPr}^i_3)_2$, where in the slow-exchange ^1H NMR spectra of the partially deuterated complex the signal assigned to the HD ligand has not revealed H–D coupling.¹³ As the most probable reason for this phenomenon a fast deuterium relaxation in the HD ligand has been put forward, which prevails at low temperature and originates scalar relaxation of the second kind for the ligand proton.¹³ Our observation of an “underestimated” line width of the resonance at $\delta -1.91$ is in agreement with the expected sharpening of an HD resonance when the scalar relaxation becomes more efficient.¹⁴

Another surprising feature of the spectra at 158 K (Figure 8) is the presence of additional resonances of low intensity: a triplet at $\delta -2.67$ ($^2J_{\text{HP}} = 25.5$ Hz), together with a broad line at $\delta -2.08$. It should be noted that the triplet is subjected to a small isotopic shift of -46 ppb (for the intensive triplet the shift is equal to -41 ppb) and the broad line is observable only in the case of a deuterated sample. It is plausible to suggest that protonation of $\text{ReH}_2(\text{CO})(\text{NO})(\text{PPr}^i_3)$ yields a mixture of two isomers (Chart V). From a theoretical point of view this seems to be feasible, because both CO and NO are strong π -acceptor ligands favoring

(12) Hund, H. U.; Ruppli, Berke, H. *Helv. Chim. Acta*, in press.

(13) Gusev, D. G.; Vymenits, A. B.; Bakhmutov, V. I. *Inorg. Chem.* **1992**, *31*, 1.

(14) Abragam, A. *The Principles of Nuclear Magnetism*; Oxford University: New York, 1971.

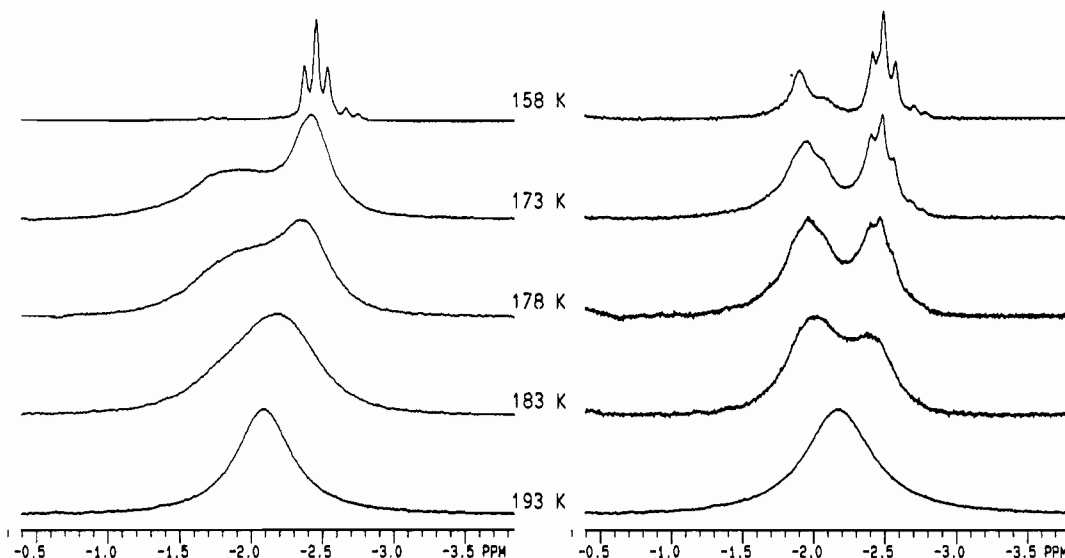
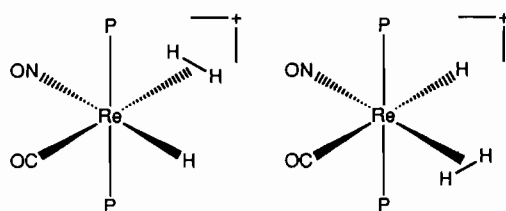


Figure 8. Hydride region of the temperature-dependent ^1H NMR spectra of **5** (left set) and a mixture of isotopomers of complex **5** formed by reaction of $\text{ReH}_2(\text{CO})(\text{NO})(\text{POPri}_3)_2$ with CF_3COOD .

Chart V



5

the formation of nonclassical hydride complexes in trans position to them.^{4,15} Attempts to find further experimental support for this situation by ^{31}P NMR have failed, however. A slightly broadened singlet at δ 39 is observed in the $^{31}\text{P}(^1\text{H})$ NMR spectrum of **5** at low temperature. Unfortunately this can result from both a small difference in chemical shifts of the existing isomers as well as from an exchange between these.

The product of protonation of $\text{ReH}_2(\text{CO})(\text{NO})(\text{PPri}_3)_2$ is unstable and decomposes with irreversible evolution of H_2 at temperatures above 200 K.

Conclusion

Protonation of a series of rhenium hydride complexes, $\text{ReH}(\text{CO})_n(\text{PMe}_3)_{5-n}$ ($n = 1-3$), $\text{ReH}_3(\text{CO})(\text{PMe}_3)_3$, and ReH_2-

$(\text{CO})(\text{NO})(\text{PPri}_3)_2$, at low temperature results in formation of products containing a dihydrogen ligand. In the case of $\text{Re}(\text{H}_2)(\text{CO})(\text{PMe}_3)_4^+$ an irreversible isomerization into a corresponding isolable cationic dihydride occurs. The other dihydrogen complexes are very labile and decompose at temperatures above 250 K with evolution of H_2 . Reasonable structures have been suggested for all of these species, and a simple mechanism for the intramolecular dynamic process in $\text{Re}(\text{H})_2(\text{H}_2)(\text{CO})(\text{PMe}_3)_3^+$ has been derived from kinetic and spectroscopic data.

Out of the two cases, protonation of $\text{ReH}(\text{CO})_2(\text{PMe}_3)_3$ and $\text{ReH}_3(\text{CO})(\text{PMe}_3)_3$, for which formation of an equilibrium mixture of classical and nonclassical complexes could be expected from observations for related compounds,² only the protonation of the trihydride yields a mixture being similar to that prepared from $\text{ReH}_3(\text{CO})(\text{PMe}_2\text{Ph})_3$.^{2a,b} This result contradicts the expected trend of increasing stability of a classical tautomer when the donating ability of PR_3 ligands increases. For both cases a H_2 moiety located trans to a CO group is assumed, showing an unpredictable dependence of the dihydride-dihydrogen equilibria on the nature of the cis PR_3 ligands.

Acknowledgment. We thank the Swiss National Science Foundation for financial support.

Supplementary Material Available: For $\text{ReH}_3(\text{CO})(\text{PMe}_3)_3$, $\text{ReH}(\text{CO})_2(\text{PMe}_3)_3$, and $[\text{ReH}_2(\text{CO})(\text{PMe}_3)_4][\text{BPh}_4]$, tables of structure determination summaries, Tables S3, S7, and S11, listing anisotropic displacement parameters, Tables S4, S8, and S12, listing H atom coordinates, Tables S1, S5, and S9, listing bond lengths, and Tables S2, S6, and S10, listing bond angles (24 pages). Ordering information is given on any current masthead page.

(15) Burdett, J. K.; Phillips, J. R.; Pourian, M. R.; Poliakoff, M.; Turner, J. J.; Upmacis, R. K. *Inorg. Chem.* **1987**, *26*, 3054.